Available online at www.sciencedirect.com
SCIENCE DIRECT®
Fluid Phase Equilibria 231 (2005) 84–98
FLUID PHASE EQUILIBRIA
www.elsevier.com/locate/fluid

Generalised virial equation of state for natural gas systems

J.F. Estela-Uribe*, J. Jaramillo

Facultad de Ingeniería, Universidad Javeriana – Cali, Calle 18118-250, Cali, Colombia

Received 5 May 2004; received in revised form 27 December 2004; accepted 13 January 2005

Abstract

In this work we present a generalised virial equation of state for natural gas systems under custody transfer conditions. The model is based on corresponding states expressions for the second and third virial coefficients with argon as the reference fluid. These functional forms involve 12 adjustable coefficients. For the extension to mixtures we propose a one-fluid mixture model with binary interaction parameters in the combining rules for the mixture critical temperature and density. We obtained overall average absolute deviations (AAD) of 0.04 and 0.08% in pure-fluid compression factors and speeds of sound; AADs of 0.07 and 0.19% in compression factors and speeds of sound, respectively, of binary mixtures and AADs of 0.047, and 0.13% in natural gas compression factors and speeds of sound, respectively. These results compare favourably with equivalent calculations with other generalised virial coefficient models.

Keywords: Virial equation of state; Virial coefficients; Density; Compression factor; Speed of sound

1. Introduction

In a previous communication, Estela-Uribe et al. [1] presented a virial equation of state (Eos) for the accurate prediction of thermodynamic properties of natural gas systems in the custody transfer regime, i.e. $270 \leq T/\mathrm{K} \leq 330$ and $p/\mathrm{MPa} \leq 12$. The model presented [1] was a virial EoS truncated at the third virial coefficient with the second, B, and third, C, virial coefficients given as quadratic functions of $1/T$ and the mixture virial coefficients were obtained from interaction virial coefficients through formal mixing rules. The results obtained were quite satisfactory in comparison with those yielded by reference models for natural gas applications, namely the GERG virial EoS [2] and the AGA8-DC92 model [3]. The overall average absolute deviation (AAD) in densities of natural gases was 0.034% and the AAD in speeds of sound was 0.17%.

The development of a virial EoS for natural gas systems requires knowledge of large numbers of interaction virial coefficients. Thus, for a typical 13-component natural gas system, virial coefficients are needed for 546 different interactions. However, given the very small mole fractions of some components in those mixtures, GERG estimated [2] that cross virial coefficients would be needed for about a hundred different interactions. Indeed, the virial EoS of [1] is based on cross virial coefficients for 106 different interactions comprising second and third virial coefficients for 12 like interactions, second virial coefficients for 24 unlike interactions and third virial coefficients for 58 unlike interactions.

To reduce the amount of substance- and interaction-specific information required, our interest in this work is to develop a generalised virial EoS for application to natural gas systems under the custody transfer regime, with the subsidiary interest of applying this model to a wider variety of non-polar compounds. Generalised virial equations are based on the corresponding states principle (CSP) given the direct connection between the intermolecular potential and the virial coefficients. Thus, it is possible to formulate expressions for B and C in terms of the CSP as universal functions of the reduced temperature. Common examples of such models are those of Tsonopoulos [4] for the reduced second virial coefficient and of Orbey and Vera [5] for the reduced third virial coefficient.

* Corresponding author. Tel.: +57 2 3218390; fax: +57 2 5552180.
E-mail address: jfe@puj.edu.co (J.F. Estela-Uribe).

0378-3812/$ – see front matter © 2005 Elsevier B.V. All rights reserved.
doi:10.1016/j.fluid.2005.01.005

In our work we shall compare the model we propose with those of [4,5] with extension to mixtures as recommended by Prausnitz et al. [6]. We shall show that it is possible to improve the predictive capability of the model while reducing the number of adjustable coefficients. On the other hand, our proposed mixture model improves on the common method of using mixing rules to obtain the pseudo-reduced properties of binary interactions in a mixture [6]. We shall argue that the proposed method leads to a significant improvement on the calculation of properties of multicomponent mixtures. We shall also report on deviations in calculated B and C, densities and speeds of sound of pure components and binary mixtures.

2. Theory

The virial equation stands as one of the most elegant yet easy-to-use EoS because of its sound foundation on the statistical-mechanical theory. Formally, the virial equation is obtained from a series expansion of either the radial distribution function or the grand canonical partition function for low-density gases. The virial coefficients are directly associated with the intermolecular potential energy so that B is related to the energy of interaction between pairs of molecules, C is related to the energy of interaction between triplets of molecules, and so forth. Also, the mixture virial coefficients are derived directly from theory so that there is no need, in principle, to resort to empirical combining rules.

There is no clear theoretical indication for the convergence of the virial EoS. Yet, the results of the models of [1,2] indicate that virial equations truncated at C can represent the densities of gas mixtures up to one-third of the critical density. As the densities of natural gas systems under custody transfer operations rarely exceed one-third of the critical density even at the lowest temperature and highest pressure, i.e. $T = 270\,\mathrm{K}$ and $p = 12\,\mathrm{MPa}$, we shall use a virial EoS truncated at C. Thus, the mixture compression factor Z is given by

$$Z = 1 + B_{\mathrm{mix}}\rho_n + C_{\mathrm{mix}}\rho_n^2. \tag{1}$$

Here, ρ_n is the amount-of-substance density and B_{mix} C_{mix} are the mixture second and third virial coefficients given by the relations:

$$B_{\mathrm{mix}} = \sum_i \sum_j x_i x_j B_{ij}, \tag{2}$$

$$C_{\mathrm{mix}} = \sum_i \sum_j \sum_k x_i x_j x_k C_{ijk}. \tag{3}$$

In Eqs. (2) and (3), x_i, x_j and x_k are the mole fractions of the i-th, j-th and k-th components of the mixture; B_{ij} and C_{ijk} are, respectively, the interaction second and third virial coefficients that are functions of temperature only.

In practice, the availability of information about B_{ij} and C_{ijk} is a limitation for the use of Eqs. (2) and (3). For instance, in the case of a 13-component natural gas mixture, Eqs. (2) and (3) involve 546 different interactions, for many of which it is not possible to associate reliable interaction virial coefficients. However, as the mole fractions of hydrocarbons higher than propane are very small, the numerical effect on B_{mix} and C_{mix} of interactions containing those components is negligible. This allows for the reduction in the amount of significant interactions to around a hundred as already shown [1,2]. Nevertheless, as in the models of [1,2], each B_{ij} and C_{ijk} depends on temperature through 3-term polynomials, this results in models that incorporate on the order of 300 adjustable coefficients. The number of adjustable coefficients would be nearly the same, or even greater, should the virial coefficients be calculated by integration of model intermolecular potentials. To reduce the number of coefficients, an alternative is to use generalised virial coefficients.

From the direct connection between the virial coefficients and the intermolecular potential, the CSP can be extended to virial coefficients. For spherically symmetrical molecules, the intermolecular potential u is given by

$$u(r) = \varepsilon\Phi\left(\frac{r}{\sigma}\right), \tag{4}$$

where r is the separation between molecules, ε the energy at the potential-energy minimum, σ the separation at which the potential energy is zero, and Φ a function of distance only. From Eq. (4) it follows that the dimensionless (or reduced) potential energy is a function only of the dimensionless separation:

$$u^*(r) = \Phi(r^*). \tag{5}$$

where $u^* = u/\varepsilon$ is the dimensionless potential energy and $r^* = r/\sigma$ is the dimensionless separation. On the other hand, the second virial coefficient can be expressed in terms of dimensionless variables as

$$B = -2\pi N_{\mathrm{A}}\sigma^3 \int_0^\infty \left[\exp\left(\frac{-\varepsilon\Phi(r^*)}{k_{\mathrm{B}}T}\right) - 1\right] r^{*2}\mathrm{d}r^* \tag{6}$$

in which N_{A} is Avogadro's constant and k_{B} is Boltzmann's constant. By setting $\varepsilon/k_{\mathrm{B}}$ proportional to the critical temperature T^{c}, the reduced second virial coefficient $B^* = B^*/2\pi N_{\mathrm{A}}\sigma^3$ is

$$B^* = \Phi_{\mathrm{B}}(T_{\mathrm{r}}). \tag{7}$$

where Φ_{B} is a universal function only of the reduced temperature $T_{\mathrm{r}} = T/T^{\mathrm{c}}$.

As the CSP is formally correct only for spherical molecules, Eq. (7) would not be accurate for fluids that deviate from spherical symmetry. One of the methods used to improve the application of the CSP to fluids of non-spherical geometry is the three-parameter CSP. This method is a perturbation on the CSP with the introduction of a parameter characterising the non-symmetrical geometry of the molecule. The most common characterising parameter is Pitzer's acentric factor [7]. Thus, Eq. (7) could be extended to fluids with

non-spherical geometry as

$$B = \left(\frac{RT^{c}}{p^{c}}\right)[B_0(T_r) + (\omega - \omega_0)B_1(T_r)], \quad (8)$$

in which B_0 represents the reduced second virial coefficient of a simple, i.e. spherical, fluid, B_1 accounts for the contribution due to the non-spherical geometry of the fluid of interest and ω and ω_0 are, respectively, the acentric factors of the fluid of interest and the reference fluid. The correlations by Tsonopoulos [4], Orbey [8], Kis and Orbey [9], Schreiber and Pitzer [10] and Pitzer [11] are examples of Eq. (8) but use $\omega_0 = 0$.

In the case of the third virial coefficient it is necessary to account for the pairwise and non-additive contributions to the intermolecular potential energy. A corresponding states model would be appropriate only for the pairwise contribution. However, the non-additive contribution is important only at low reduced temperatures [6]. Thus, a correlation for the third virial coefficient would be analogous to that of Eq. (8) as

$$C = \left(\frac{RT^{c}}{p^{c}}\right)^{2}[C_0(T_r) + (\omega - \omega_0)C_1(T_r)]. \quad (9)$$

The correlations by Chueh and coworkers [12] and Orbey and Vera [5] are examples of Eq. (9) with $\omega_0 = 0$. For convenience, we reproduce in Appendix A the correlations of Tsonopoulos [4] and Orbey and Vera [5].

Corresponding states models are formulated for fluids whose configurational properties are described by classical mechanics. For low-molecular weight molecules at low temperatures, quantum-mechanical effects are significant, such that corresponding states models do not apply under those conditions. Gunn et al. [12] outlined a technique whereby temperature-dependent effective critical constants are used in corresponding states models for the quantum gases H_2, He and Ne. In our work it is necessary to include those corrections because H_2 and He are components of natural gas mixtures.

The extension to mixtures is possible given the equivalence between the intermolecular potential parameter and the critical constants in the CSP, so that combining rules for the intermolecular potential parameters are extended, by analogy, to combining rules for pseudo-critical constants. Thus, to calculate B_{ij} one can replace T^c, p^c and ω in Eq. (8) with T^c_{ij}, p^c_{ij} and ω_{ij}, respectively, and use $T_{r,ij} = T/T^c_{ij}$. Lee and Kesler [13] proposed combining rules for the pseudo-critical properties, which are reproduced in Appendix A, where we also present the approximation proposed by Orentlicher and Prausnitz [14] for the interaction third virial coefficient C_{ijk}.

3. Proposed model

The model we propose is based on Eqs. (8) and (9) with the functions B_0, B_1, C_0 and C_1 given by

$$B_0(T_r) = b_{0,1} + \frac{b_{0,2}}{T_r^{1.5}} + \frac{b_{0,3}}{T_r^{2}}, \quad (10)$$

$$B_1(T_r) = b_{1,1} + \frac{b_{1,2}}{T_r^{2.5}} + \frac{b_{1,3}}{T_r^{3}}, \quad (11)$$

$$C_0(T_r) = c_{0,1} + \frac{c_{0,2}}{T_r^{2.5}} + \frac{c_{0,3}}{T_r^{10}}, \quad (12)$$

and

$$C_1(T_r) = c_{1,1} + \frac{c_{1,2}}{T_r^{8}} + \frac{c_{1,3}}{T_r^{10}}. \quad (13)$$

Thus, the model incorporates 12 adjustable coefficients whereas the Tsonopoulos [4] and Orbey and Vera [5] correlations use 17 adjustable coefficients altogether. We chose argon as the reference fluid because this is an almost spherical molecule and calculated $\omega_0 = -0.002202$ with the ancillary vapour pressure equation from Tegeler et al. [15]. The value of ω_0 is very small but it is not null nonetheless. In fact, ω_0 need not be zero and this allows for flexibility in the choice of the reference fluid according to the class of fluids of interest.

The coefficients of Eqs. (10)–(13) were fitted against a data set comprising 969 compression-factor data and 231 speed of sound data for natural gas components in the intervals $270 \leq T/\mathrm{K} \leq 330$ and $p/\mathrm{MPa} \leq 12$. The compression factors were taken from the GERG 1990 Databank [16] for CH_4, C_2H_6, C_3H_8, N_2, CO_2, CO, H_2 and He. Speeds of sound were taken from the data by Trusler and Zarari [17] for CH_4; Estrada-Alexanders and Trusler [18] for C_2H_6; Trusler and Zarari [19] for C_3H_8; Boyes [20], Ewing and Trusler [21] and Costa-Gomes and Trusler [22] for N_2 and Estrada-Alexanders and Trusler [23] for CO_2. In Table 1 we give the optimised coefficients.

For the extension to mixtures we propose a one-fluid mixture model instead of the method outlined in Appendix A. We argue that the drawback of the method of Eqs. (A.10)–(A.18) is the approximation to C_{ijk} of Eq. (A.18). For binary mixtures the effect of the approximation might be small, yet for multicomponent systems the cumulative effect may become significant. On the other hand, the correlation of Eq. (A.13) is formally unsatisfactory because in the pure-component limit it does not converge to the critical compression factor given by the relationship $Z^c_i = p^c_i/(\rho^c_i RT^c_i)$. In the method we propose, the mixture is characterised by pseudo-critical constants, the mixing of critical properties is carried out once and the mixture virial coefficients are calculated with Eqs. (8) and (9) as if the mixture were a single component. We take the expressions proposed by Clarke [24] for the mixture

Table 1
Coefficients of functions B_0, B_1, C_0 and C_1 of Models 1 and 2

Coefficient	Value	Coefficient	Value
$b_{0,1}$	0.11993755	$c_{0,1}$	0.00856591
$b_{0,2}$	−0.57931684	$c_{0,2}$	0.03621018
$b_{0,3}$	0.12468363	$c_{0,3}$	−0.00791697
$b_{1,1}$	0.06783874	$c_{1,1}$	−0.02124512
$b_{1,2}$	0.98723789	$c_{1,2}$	0.05884014
$b_{1,3}$	−1.09259643	$c_{1,3}$	−0.02040829

critical density ρ_x^c and critical temperature T_x^c:

$$\rho_x^c = \left[\sum_i \sum_j \frac{x_i x_j}{\rho_{ij}^c}\right]^{-1}, \tag{14}$$

and

$$T_x^c = \rho_x^c \sum_i \sum_j \frac{x_i x_j T_{ij}^c}{\rho_{ij}^c}. \tag{15}$$

In Eqs. (14) and (15) the subscript "x" indicates mixture properties. For the interaction critical density ρ_{ij}^c we propose the following modified form of Eq. (A.11):

$$\rho_{ij}^c = 8(1+d_{ij})^{-3}\left[\left(\frac{1}{\rho_i^c}\right)^{1/3} + \left(\frac{1}{\rho_j^c}\right)^{1/3}\right]^{-3}. \tag{16}$$

where d_{ij} is a binary interaction parameter. For T_{ij}^c in Eq. (15) we use Eq. (A.10), in which each T_i^c is given by Eq. (A.7) if any of the components of the interaction is H_2 or He. For the interaction parameter k_{ij} of Eq. (A.10) we use the expression proposed by Walas [25]:

$$k_{ij} = 1 - \frac{a_{ij}\rho_{ij}^c}{(\rho_i^c \rho_j^c)^{1/2}} \tag{17}$$

in which we have introduced the binary interaction parameter a_{ij}. The pseudo-critical pressure of the mixture p_x^c is obtained from

$$p_x^c = Z_x^c \rho_x^c R T_x^c \tag{18}$$

For the mixture critical compression factor Z_x^c we use the mole-weighted average:

$$Z_x^c = \sum_i x_i Z_i^c \tag{19}$$

in which the individual component critical compression factors are obtained from $Z_i^c = p_i^c/(\rho_i^c R T_i^c)$, where the corrections of Eqs. (A.7)–(A.9) are used for quantum components. For the mixture acentric factor we use the number average:

$$\omega_x = \sum_i x_i \omega_i. \tag{20}$$

Thus, in the proposed method, T^c, p^c and ω of Eqs. (8) and (9) are replaced with T_x^c, p_x^c and ω_x, respectively, and T_r is given by $T_r = T/T_x^c$. In addition, there is no need to use Eqs. (2) and (3) and the approximation to C_{ijk} of Eq. (A.18) because the virial coefficients of Eqs. (8) and (9) can be used directly in Eq. (1) for the mixture compression factor. This, however, is an approximation to the formal mixture virial coefficients of Eqs. (2) and (3) because the composition dependence of the proposed one-fluid model is different from the simple quadratic and cubic functionalities of the formal mixture virial coefficients. Finally, Eqs. (14)–(20) reduce naturally to single-component expressions in the pure-component limit.

To ensure thorough analysis of the results given by the proposed functionalities for the generalised virial coefficients and the mixture model, we shall compare the following four models. Model 1 is the basic proposal of this work, i.e. the generalised virial coefficients of Eqs. (8)–(13) and the one-fluid mixture model of Eqs. (14)–(20). Model 2 is based on Eqs. (8)–(13) with the mixture model of Eqs. (A.10)–(A.18); however, Eq. (A.13) is changed to:

$$Z_{ij}^c = \tfrac{1}{2}(Z_i^c + Z_j^c), \tag{21}$$

to ensure consistency in the pure-component limit. Model 3 is based on the Tsonopoulos [4] and Orbey and Vera correlations [5], i.e. Eqs. (A.1)–(A.6), and the mixture model of Eqs. (14)–(20). Finally, Model 4 is based on Eqs. (A.1)–(A.6) and the mixture model of Eqs. (A.10)–(A.18) but with Eq. (21) replacing Eq. (A.13). Thus, the effect of the virial coefficient model is analysed from the comparison of Model 1–3 and Model 2–4, whereas the effect of the mixture model is analysed from the comparison of Model 1–2 and Model 3–4. In the four models ρ_{ij}^c and k_{ij} are given by Eqs. (16) and (17). To fit the binary interaction parameters d_{ij} and a_{ij} of Eqs. (16) and (17) we used only the binary-mixture compression factor data reported in the GERG 1990 Databank [16] because these state-of-the-art measurements have been critically assessed with regards to experimental technique and internal consistency and are claimed to be accurate within ±0.1%. In Table 2 we present the values of d_{ij} and a_{ij} optimised for the 19 unlike interactions that correspond to the mixtures for which there are data in [16]. For like interactions, and for mixtures not listed in Table 2, the binary interaction parameters have the default values $d_{ij} = 1$ and $a_{ij} = 0$.

4. Results and discussion

4.1. Results

The results we present are deviations in calculated compression factors and speeds of sound of pure components, binary mixtures and natural gas systems. In addition, we report deviations in calculated second and third virial coefficients of pure components and binary mixtures. Compression factors for both pure fluids and mixtures were calculated with the proposed four models as outlined in Section 3. Speeds of sound in the thermodynamic limit were calculated with the relation:

$$u^2 = \left(\frac{RT}{M}\right)\left[Z + \rho_n\left(\frac{\partial Z}{\partial \rho_n}\right)_T + \frac{R}{C_V}\left(Z + T\left(\frac{\partial Z}{\partial T}\right)_{\rho_n}\right)^2\right]. \tag{22}$$

In Eq. (21) M is the mole weight of the component, or the mixture, and C_V is the isochoric heat capacity given by

Table 2
Binary interaction parameters d_{ij} and a_{ij} of Models 1–4

Interaction	Model 1		Model 2	
	d_{ij}	a_{ij}	d_{ij}	a_{ij}
CH_4—C_2H_6	1.023000	0.002524	1.008085	0.003361
CH_4—C_3H_8	1.108130	0.045592	0.997028	0.001572
CH_4—i-C_4H_{10}	1.178450	0.064475	1.071740	0.035076
CH_4—n-C_4H_{10}	1.064020	0.021620	0.966976	−0.010767
CH_4—n-C_5H_{12}	1.064110	0.001510	0.982959	−0.013338
CH_4—n-C_6H_{14}	1.353330	0.116272	1.348887	0.120782
CH_4—N_2	1.037100	0.022402	1.025344	0.021365
CH_4—CO_2	0.945619	−0.017417	0.977654	0.016505
CH_4—CO	1.094280	0.034345	0.978114	−0.003841
CH_4—H_2	1.077400	0.000578	0.941270	−0.021147
C_2H_6—H_2	1.100260	−0.016260	0.909185	−0.029291
N_2—C_2H_6	1.008970	−0.002350	0.990525	0.018254
N_2—C_3H_8	1.255540	0.123985	1.119823	0.081907
N_2—n-C_4H_{10}	1.594740	0.271224	1.416704	0.209650
N_2—CO_2	1.103340	0.011300	1.093940	0.039339
N_2—CO	1.660890	0.205654	1.588611	0.187300
N_2—H_2	1.038660	0.016725	0.997903	0.006113
CO_2—C_2H_6	0.918546	−0.000233	0.914012	−0.002415
CO_2—H_2	1.274400	−0.015689	1.008490	−0.015459
	Model 3		Model 4	
CH_4—C_2H_6	1.045560	0.020230	1.011163	0.009477
CH_4—C_3H_8	1.061350	0.025907	0.977225	−0.006413
CH_4—i-C_4H_{10}	1.163460	0.063835	1.073109	0.040598
CH_4—n-C_4H_{10}	0.873445	−0.090245	0.783299	−0.108329
CH_4—n-C_5H_{12}	0.823402	−0.050224	0.821792	−0.032702
CH_4—n-C_6H_{14}	0.533503	−0.254636	0.925981	0.046424
CH_4—N_2	0.969196	−0.001213	0.948983	−0.005744
CH_4—CO_2	0.953184	−0.009268	0.973536	0.017292
CH_4—CO	0.808028	−0.059617	0.773634	−0.071862
CH_4—H_2	0.995171	−0.020076	0.856162	−0.050322
C_2H_6—H_2	1.014940	−0.041472	0.868729	−0.051502
N_2—C_2H_6	1.051790	0.018719	0.982952	0.018279
N_2—C_3H_8	1.056030	0.044053	0.898457	−0.012433
N_2—n-C_4H_{10}	0.966362	0.033034	0.876466	0.001142
N_2—CO_2	1.045270	−0.010767	1.002676	0.003146
N_2—CO	0.853647	0.001041	0.857115	0.002619
N_2—H_2	0.890320	−0.017817	0.795587	−0.045321
CO_2—C_2H_6	0.927895	0.008793	0.922916	0.007118
CO_2—H_2	1.278000	−0.012118	0.911990	−0.050324

$C_V = C_V^{pg} + C_V^{res}$, in which the perfect-gas contribution C_V^{pg} is obtained with the generalised correlation by Jaeschke and Schley [26] and the residual contribution C_V^{res} is given by

$$\left(\frac{C_V^{res}}{R}\right) = -\left[2T\left(\frac{dB}{dT}\right) + T^2\left(\frac{d^2B}{dT^2}\right)\right]\rho_n - \left[T\left(\frac{dC}{dT}\right) + \frac{T^2}{2}\left(\frac{d^2C}{dT^2}\right)\right]\rho_n^2. \quad (23)$$

Estela-Uribe et al. [1] showed that the calculation of speeds of sound with a virial EoS is significantly improved when the temperature dependence of the virial coefficients is such that the first and second temperature derivatives of B and C are functions of temperature. Clearly, the functionalities in $1/T$ of Eqs. (10)–(13) satisfy this condition.

Table 3
Summary of percentage average absolute deviations in calculated compression factors and speeds of sound of pure fluids

Fluid	References	Number of points	Models 1 and 2	Models 3 and 4
Z				
CH_4	[16]	821	0.032	0.052
C_2H_6	[16]	189	0.040	0.236
C_3H_8	[16]	26	0.038	0.131
N_2	[16]	512	0.058	0.096
CO_2	[16]	418	0.029	0.104
CO	[16]	15	0.076	0.037
H_2	[16]	130	0.032	0.192
He	[16]	127	0.051	0.470
Overall		2238	0.040	0.120
u				
CH_4	[17]	48	0.179	0.142
C_2H_6	[18]	88	0.081	0.524
C_3H_8	[19]	30	0.041	0.090
N_2	[20–22]	121	0.054	0.034
CO_2	[23]	20	0.058	0.198
Overall		307	0.080	0.207

In Tables 3–5 we present deviations in compression factors and speeds of sound calculated with the four models together with the sources of experimental data. The statistic we used was the percentage AAD. The results of Table 3 are for pure components; those of Table 4 are for binary mixtures and those of Table 5 are for natural gas systems. In Table 3, the results of Models 1 and 2 are the same, as well as those of Models 3 and 4, because the mixture models of Eqs. (14)–(20) and (A.10)–(A.18) reduce to the single-component critical properties. For the results of Table 5, experimental compression factors were taken from [16] for the samples denominated Groups 1–6 and from [32,33] for the samples denominated GU1, GU2, RG2, NIST1 and NIST2. Gases of Groups 1–6 comprise 84 different gas samples. Those groups were classified by GERG [2] such that Group 1 gases have $x_{N_2} > 0.095$ and $x_{H_2} = 0$; Group 2 gases have $x_{CO_2} > 0.04$; gases of Group 3 have $x_{C_2H_6} > 0.08$; gases of Group 4 have $x_{H_2} > 0.02$; Group 5 gases have $x_{N_2} > 0.04$ and $x_{C_2H_6} > 0.04$; and Group 6 gases have $x_{CH_4} > 0.94$. The compositions reported in [32,33] indicate that samples GU1, GU2, RG2 and NIST1 correspond to gases of Groups 1–3 and 6, respectively. Sample NIST 2 is similar to Group 5 gases. The gas samples of [27] are named according to geographical origin, and the sample denominated Synthetic is a five-component synthetic mixture [29]. In Table 6 we summarise the results of the four models regarding pure components, binary mixtures and natural gas mixtures.

In Figs. 1–7 we present results only for Model 1. In Figs. 1 and 2 we present percentage deviations in compression factors and speeds of sound, respectively, for CH_4, N_2 and CO_2. In Figs. 3 and 4 we present percentage deviations in compression factors and speeds of sound, re-

Table 4
Summary of percentage average absolute deviations in calculated compression factors and speeds of sound of binary mixtures

System	References	No. of points	Model 1	Model 2	Model 3	Model 4
Z						
(CH_4+C_2H_6)	[16]	794	0.045	0.038	0.046	0.056
(CH_4+C_3H_8)	[16]	217	0.021	0.069	0.028	0.042
(CH_4+*i*-C_4H_{10})	[16]	27	0.016	0.045	0.018	0.044
(CH_4+*n*-C_4H_{10})	[16]	192	0.042	0.052	0.038	0.051
(CH_4+*n*-C_5H_{12})	[16]	21	0.021	0.023	0.015	0.016
(CH_4+*n*-C_6H_{14})	[16]	119	0.035	0.034	0.036	0.037
(CH_4+N_2)	[16]	933	0.068	0.064	0.037	0.035
(CH_4+CO_2)	[16]	357	0.100	0.100	0.100	0.115
(CH_4+CO)	[16]	132	0.044	0.043	0.040	0.039
(CH_4+H_2)	[16]	404	0.038	0.023	0.040	0.047
(C_2H_6+H_2)	[16]	156	0.059	0.026	0.047	0.024
(N_2+C_2H_6)	[16]	298	0.268	0.086	0.246	0.077
(N_2+C_3H_8)	[16]	153	0.055	0.069	0.029	0.026
(N_2+*n*-C_4H_{10})	[16]	113	0.058	0.060	0.013	0.015
(N_2+CO_2)	[16]	247	0.079	0.061	0.086	0.039
(N_2+CO)	[16]	130	0.071	0.070	0.014	0.014
(N_2+H_2)	[16]	456	0.060	0.038	0.073	0.065
(CO_2+C_2H_6)	[16]	499	0.047	0.039	0.068	0.056
(CO_2+H_2)	[16]	213	0.121	0.022	0.131	0.037
Overall		5461	0.070	0.052	0.064	0.051
u						
(CH_4+C_2H_6)	[27,28,29]	340	0.198	0.998	0.358	0.375
(CH_4+C_3H_8)	[27,30]	60	0.218	0.382	0.173	0.285
(CH_4+N_2)	[27,31]	243	0.220	0.213	0.147	0.136
(CH_4+CO_2)	[27,31]	162	0.133	0.192	0.083	0.186
(N_2+CO_2)	[27]	39	0.186	0.269	0.198	0.206
Overall		844	0.193	0.540	0.224	0.255

spectively, for the systems ($CH_4 + C_2H_6$), ($CH_4 + N_2H_6$) and ($CH_4 + CO_2$). In Figs. 5 and 6 we present percentage deviations in compression factors of natural gases and speeds of sound of natural gases, respectively, and the frequency distributions of those deviations are presented in Fig. 7.

In Table 7 we present average deviations in second and third virial coefficients of pure fluids calculated with the

Table 5
Summary of percentage average absolute deviations in calculated compression factors and speeds of sound of natural gas systems

System	References	No. of points	Model 1	Model 2	Model 3	Model 4
Z						
Group 1	[16]	713	0.052	0.060	0.045	0.050
Group 2	[16]	477	0.064	0.050	0.097	0.056
Group 3	[16]	1403	0.055	0.282	0.129	0.164
Group 4	[16]	690	0.041	0.056	0.061	0.051
Group 5	[16]	660	0.039	0.082	0.065	0.064
Group 6	[16]	530	0.028	0.029	0.034	0.033
GU1	[32,33]	84	0.040	0.044	0.035	0.034
GU2	[32,33]	87	0.071	0.066	0.066	0.061
RG2	[32,33]	87	0.031	0.121	0.037	0.088
NIST1	[32,33]	84	0.029	0.033	0.026	0.028
NIST2	[32,33]	85	0.032	0.046	0.034	0.039
Overall		4900	0.047	0.122	0.078	0.084
u						
Gulf Coast	[27]	48	0.136	0.172	0.158	0.195
Amarillo	[27]	48	0.139	0.188	0.159	0.190
Statoil Dry	[27]	58	0.093	0.199	0.157	0.168
Statvordgass	[27]	27	0.160	0.229	0.133	0.227
Synthetic	[29]	10	0.148	0.272	0.133	0.195
Overall		191	0.128	0.196	0.153	0.190

Table 6
Summary of overall percentage average absolute deviations in calculated compression factors and speeds of sound of pure fluids, binary mixtures and natural gas systems

Property	No. of points	Model 1	Model 2	Model 3	Model 4
Z					
Pure fluids	2238	0.040	0.040	0.120	0.120
Binary mixtures	5461	0.070	0.052	0.064	0.051
Natural gas systems	4900	0.047	0.122	0.078	0.084
Overall	12599	0.056	0.077	0.079	0.076
u					
Pure fluids	307	0.080	0.080	0.207	0.207
Binary mixtures	844	0.193	0.540	0.224	0.255
Natural gas systems	191	0.128	0.196	0.153	0.190
Overall	1342	0.158	0.386	0.210	0.235

four models. Those deviations were calculated as $\Delta B = \frac{1}{n}\sum_{i=1}^{n}\left|B_{\mathrm{exp},i} - B_{\mathrm{calc},i}\right|$ and $\Delta C = \frac{1}{n}\sum_{i=1}^{n}\left|C_{\mathrm{exp},i} - C_{\mathrm{calc},i}\right|$. In Fig. 8 we present deviations between second virial coefficients calculated with Model 1 and the data of Gilgen et al. [35] for Ar, Kleinrahm et al. [38] and Händel et al. [39] for CH_4 and Nowak et al. [36] for N_2. In Fig. 9 we present experimental third virial coefficients for Ar [34], CH_4 [38,39] and N_2 [36] together with the corresponding third virial coefficients calculated with Model 1.

In Table 8 we present average deviations ΔB and ΔC in mixture virial coefficients calculated with Models 2 and 4. As we indicated in Section 3, the one-fluid mixture model does not allow the calculation of formal mixture virial coefficients; therefore, we do not include comparisons of results calculated with Models 1 and 3. On the contrary, as the mixture model of Eqs. (A.10)–(A.18) produce individual interaction virial coefficients, we only report results calculated with Models 2 and 4. Deviations were calculated with respect to the data by Hou et al. [47] and McElroy and Fang [48] for the system ($CH_4 + C_2H_6$); Hou et al. [47], Brugge et al. [49] and Esper et al. [50] for the system ($CH_4 + CO_2$); Achtermann et al. [51] for the system ($N_2 + C_2H_6$); Brugge et al. [49] and

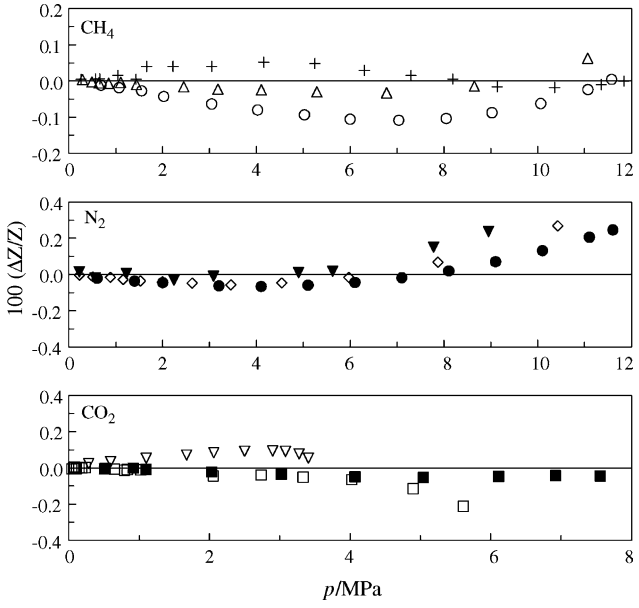

Fig. 1. Relative deviations $\Delta Z/Z$ between experimental densities from [16] and values calculated with the proposed model for pure fluids. For CH_4: (+) 273.15 K; (△) 293.15 K; (◯) 323.15 K. For N_2: (▼) 273 K; (◊) 293 K; (●) 323 K. For CO_2: (▽) 273 K; (□) 300 K; (■) 320 K.

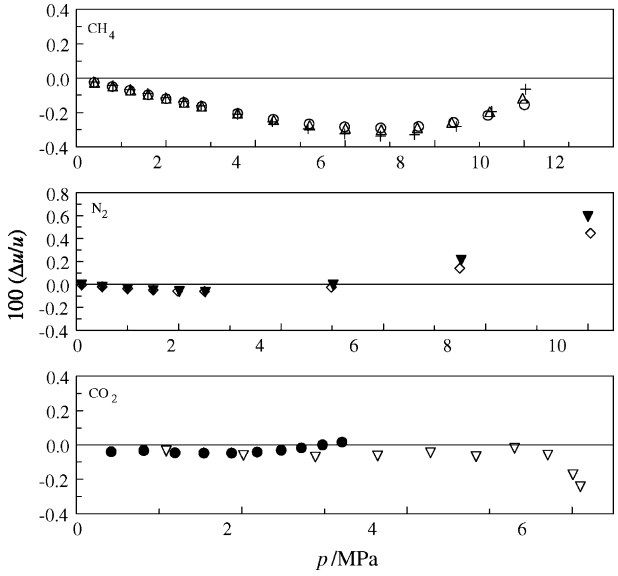

Fig. 2. Relative deviations $\Delta u/u$ between experimental speeds of sound and values calculated with the proposed model for pure fluids. For CH_4 with data from [17]: (+) 275 K; (△) 300 K; (◯) 325 K. For N_2 with data from [22]: (▼) 275 K; (◊) 300 K. For CO_2 with data from [23]: (●) 275 K; (▽) 300 K.

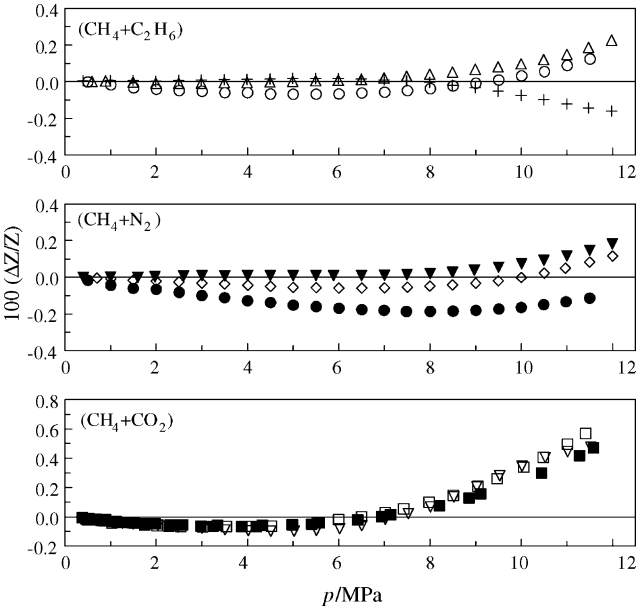

Fig. 3. Relative deviations $\Delta Z/Z$ between experimental densities from [16] and values calculated with the proposed model for binary systems. For ($0.91935CH_4 + 0.08065C_2H_6$): (+) 270 K; (△) 290 K; (◯) 330 K. For ($0.80021CH_4 + 0.19976N_2$): (▼) 270 K; (◊) 290 K; (●) 330 K. For ($0.6855CH_4 + 0.3145CO_2$): (▽) 270 K; (□) 310 K; (■) 330 K.

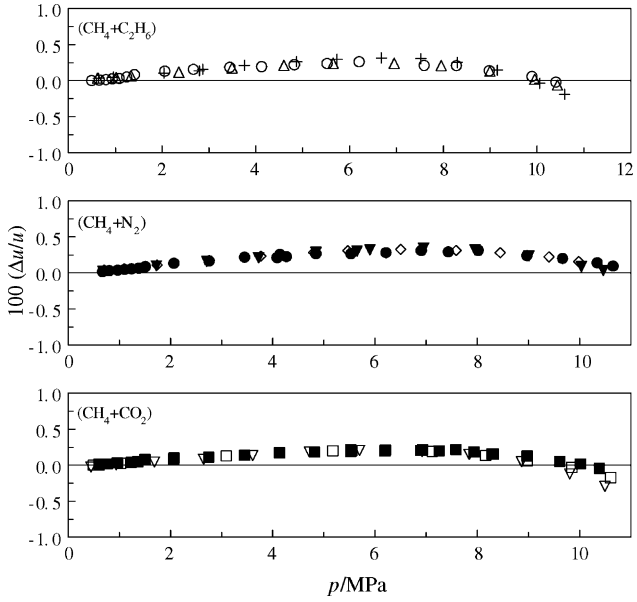

Fig. 4. Relative deviations $\Delta u/u$ between experimental speeds of sound from [27] and values calculated with the proposed model for binary systems. For ($0.94985CH_4 + 0.05015C_2H_6$): (+) 275 K; (△) 300 K; (◯) 325 K. For ($0.95114CH_4 + 0.04886N_2$): (▼) 275 K; (◊) 300 K; (●) 325 K. For ($0.94979CH_4 + 0.05021CO_2$): (▽) 275 K; (□) 300 K; (■) 325 K.

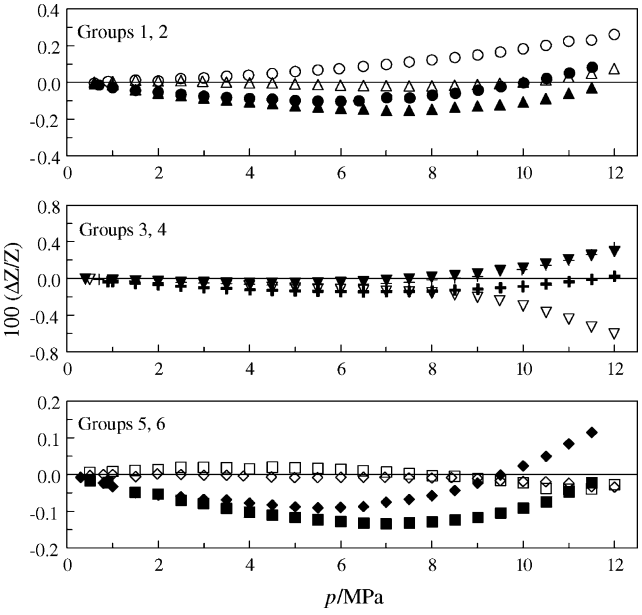

Fig. 5. Relative deviations $\Delta Z/Z$ between experimental compression factors of natural gases from [16] and values calculated with the proposed model. (△) sample N60 at 270 K; (▲) sample N60 at 330 K; (◯) sample N64 at 270 K; (●) sample N64 at 330 K; (▽) sample N66 at 270 K; (▼) sample N66 at 330 K; (+) sample N74 at 270 K; ▼ sample N74 at 330 K; (◊) sample N83 at 270 K; (♦) sample N83 at 330 K; (□) sample N62 at 270 K; (■) sample N62 at 330 K.

Esper et al. [50] for the system ($N_2 + CO_2$) and Hou et al. [47], Brugge et al. [49], McElroy et al. [52] and Weber [53] for the system ($CO_2 + C_2H_6$). In Table 9 we present average deviations ΔB_{12}, ΔC_{112} and ΔC_{122} in interaction virial

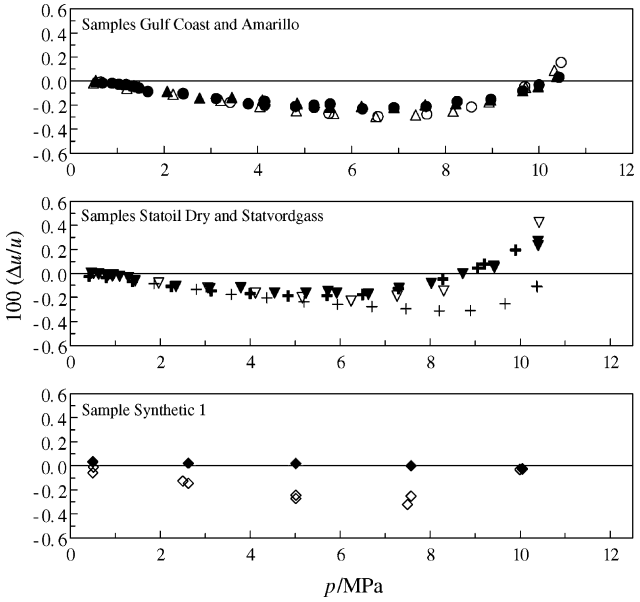

Fig. 6. Relative deviations $\Delta u/u$ between experimental speeds of sound of natural gases and values calculated with the proposed model. (△) sample Gulf Coast [27] at 275 K; (▲) sample Gulf Coast [27] at 325 K; (◯) sample Amarillo [27] at 275 K; (●) sample Amarillo [27] at 325 K; (▽) sample Statoil Dry [27] at 275 K; (▼) sample Statoil Dry [27] at 325 K; (+) sample Statvordgass [27] at 300 K; ▼ sample Statvordgass [27] at 325 K; (◊) sample synthetic [29] at 275 K; (♦) sample synthetic [29] at 300 K.

coefficients calculated with Models 2 and 4 with respect to data from references [47,49–52]. In Fig. 10 we present deviations between calculated and experimental interaction second virial coefficients of Hou et al. [47] for ($CH_4 + C_2H_6$) and ($CH_4 + CO_2$), of Esper et al. [50] for ($CH_4 + CO_2$) and

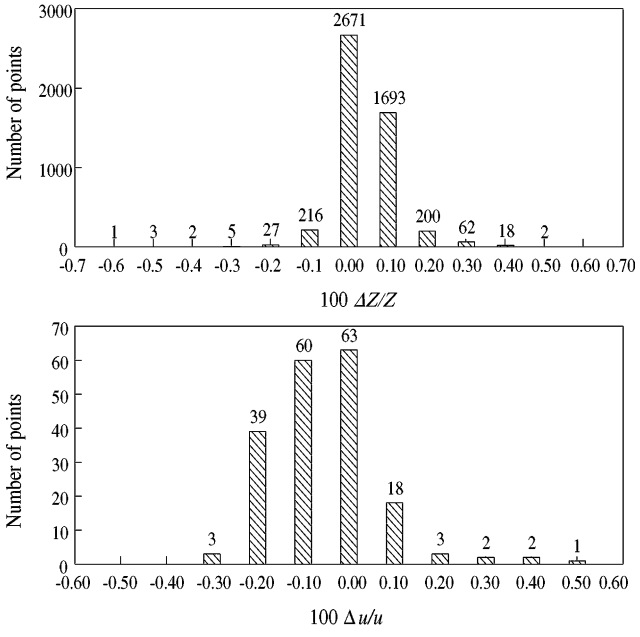

Fig. 7. Frequency distribution of deviations in compression factors of natural gas systems from [16,32,33] and values calculated with the proposed model.

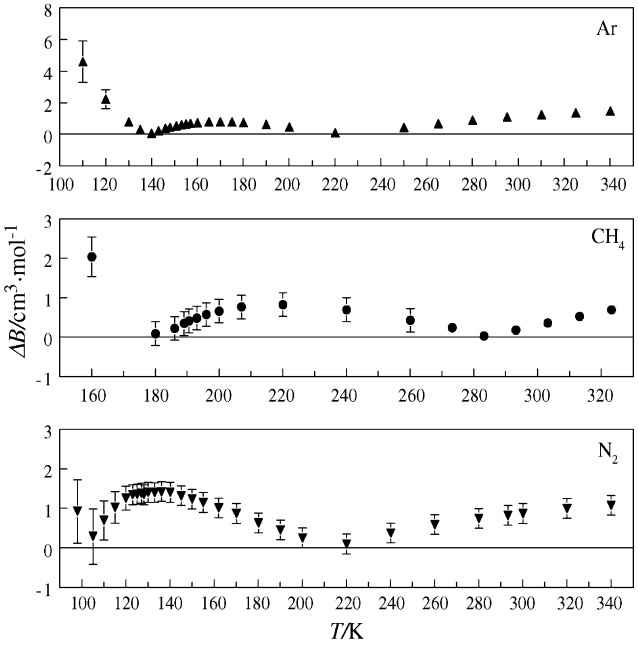

Fig. 8. Deviations between calculated and experimental second virial coefficients. (▲) for Ar with data from [35]. (●) for CH_4 with data from [38,39]. (▼) for N_2 with data from [36].

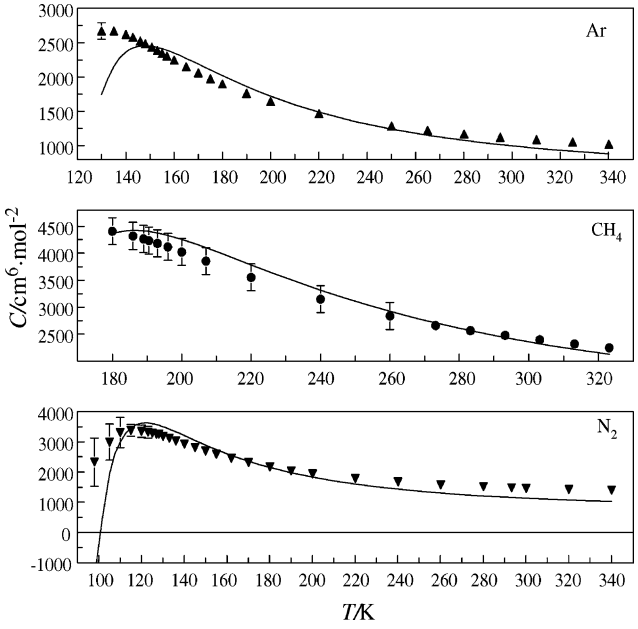

Fig. 9. Experimental and calculated third virial coefficients. (▲) data for Ar from [35]. (●) data for CH_4 from [38,39]. (▼) data for N_2 with data from [36]. (—) Values calculated with the proposed model.

Table 7
Average absolute deviations ΔB and ΔC in calculated second and third virial coefficients of pure components

Fluid	References	No. of points	Temperature interval (K)	ΔB/cm^3 mol^{-1} Models 1 and 2	ΔB/cm^3 mol^{-1} model of [4]
H_2	[34]	11	22–400	5.89	4.46
He	[34]	11	5–700	3.04	3.41
Ne	[34]	10	60–600	1.05	1.12
Ar	[35]	27	110–340	0.88	1.95
Kr	[34]	14	110–700	15.63	2.71
Xe	[34]	16	160–650	11.85	3.14
N_2	[36]	29	98–340	0.96	1.50
CO	[34]	12	213–475	2.46	1.81
CO_2	[37]	7	220–340	0.38	1.51
CH_4	[38,39]	18	160–323	0.53	0.76
C_2H_6	[40,41]	30	273–623	0.43	6.11
C_2H_4	[34]	9	240–450	0.38	1.19
C_3H_8	[42]	23	323–623	0.73	2.55
i-C_4H_{10}	[43]	8	251–320	3.53	32.20
n-C_4H_{10}	[44]	8	250–320	12.68	32.07
i-C_5H_{12}	[45]	7	260–320	4.47	83.87
n-C_5H_{12}	[46]	7	270–330	17.69	59.67
neo-C_5H_{12}	[34]	10	300–550	10.35	3.13
n-C_6H_{14}	[34]	9	300–450	43.25	21.32
C_6H_6	[34]	13	290–600	30.00	64.21
C_6H_{12}	[34]	13	300–560	31.19	64.56
Overall		292		7.59	13.64
				ΔC/cm^3 mol^{-1} Models 1 and 2	ΔC/cm^3 mol^{-1} model of [5]
Ar	[35]	25	130–340	147	76
N_2	[36]	29	98–340	388	110
CO_2	[37]	4	280–340	130	116
CH_4	[38,39]	17	180–323	131	25
C_2H_6	[40,41]	30	273–623	466	401
C_3H_8	[42]	17	343–623	843	617
Overall		108		436	272

Table 8
Absolute average deviations in second and third mixture virial coefficients calculated with the proposed models

System	Sources	No. points	Temperature range (K)	Composition range[a]	ΔB/cm^3 mol^{-1}	
					Model 2	Model 4
$CH_4 + C_2H_6$	[47,48]	19	300–343	0.3–0.7	0.80	0.78
$CH_4 + CO_2$	[47,49,50]	26	230–320	0.1–0.9	0.55	0.34
$N_2 + C_2H_6$	[51]	15	270–350	0.2–0.8	0.86	0.46
$N_2 + CO_2$	[49,50]	20	230–320	0.1–0.9	0.69	0.27
$CO_2 + C_2H_6$	[47,49,52,53]	35	300–333	0.1–0.9	1.42	1.48
Overall		115	230–350	0.1–0.9	0.92	0.76
					ΔC/cm^6 mol^{-2}	
					Model 2	Model 4
$CH_4 + C_2H_6$	[47,48]	19	300–343	0.3–0.7	180	183
$CH_4 + CO_2$	[47,49,50]	24	230–320	0.1–0.9	62	73
$N_2 + C_2H_6$	[51]	15	270–350	0.2–0.8	212	114
$N_2 + CO_2$	[49,50]	20	230–320	0.1–0.9	229	100
$CO_2 + C_2H_6$	[47,49,52,53]	35	300–333	0.1–0.9	163	171
Overall		113	230–350	0.1–0.9	163	132

[a] Mole fraction of the first component of the mixture.

($N_2 + CO_2$), of Achtermann et al. [51] for ($N_2 + C_2H_6$) and of McElroy et al. [52] for ($CO_2 + C_2H_6$).

To illustrate the difference between the mixture virial coefficients calculated with Model 2, i.e. the new virial-coefficient correlation and formal mixing rules, and the approximate values given by the one-fluid mixture model (Model 1), we show in Fig. 11 deviations calculated with both models for the data of Hou et al. [47] for ($CH_4 + CO_2$) and ($CO_2 + C_2H_6$) and Brugge et al. [49] for ($N_2 + CO_2$) at the selected isotherm of $T = 300$ K for the whole range of compositions.

4.2. Discussion

From Table 6, the comparison of Models 1–3 is quite favourable in almost all respects. The largest proportional decrease in AADs was for pure-fluid properties. Also, there was a large relative decrease for the overall AADs in natural-gas compression factors. Smaller relative reductions occurred for binary-mixture and natural-gas speeds of sound. By contrast, there was a slight increase in the overall AAD of binary-mixture compression factors.

The calculation of pure-fluid properties with Models 2 and 4 yields exactly the same AADs as that with Models 1 and 3, respectively, because the mixture models reduce formally to single-component expressions in the pure-component limit. On the other hand, the overall comparison of Models 2–4 is much less favourable. Firstly, there was a marginal increase in the overall AAD for binary-mixture compression factors. However, there occurred an important increase in the overall AAD for natural-gas Z's. From Table 5 we see that the

Table 9
Absolute average deviations in second and third interaction virial coefficients calculated with the proposed models

System	Sources	No. points	Temperature range (K)	ΔB_{12}/cm^3 mol^{-1}			
				Model 2	Model 4		
$CH_4 + C_2H_6$	[47]	2	300–320	0.84	0.19		
$CH_4 + CO_2$	[47,49,50]	14	230–320	1.12	0.83		
$N_2 + C_2H_6$	[51]	5	270–350	1.57	1.16		
$N_2 + CO_2$	[49,50]	13	230–320	1.81	1.05		
$CO_2 + C_2H_6$	[47,49,52]	8	300–333	1.14	1.84		
Overall		40	230–350	1.38	1.10		
				ΔC_{112}/cm^6 mol^{-2}		ΔC_{122}/cm^6 mol^{-2}	
				Model 2	Model 4	Model 2	Model 4
$CH_4 + C_2H_6$	[47]	2	300–320	106	145	137	171
$CH_4 + CO_2$	[47,49]	4	300–320	86	33	21	78
$N_2 + C_2H_6$	[51]	5	270–350	602	296	177	471
$N_2 + CO_2$	[49]	2	300–320	196	123	153	24
$CO_2 + C_2H_6$	[47,49,52]	8	300–333	514	466	512	560
Overall		19	270–350	384	280	269	359

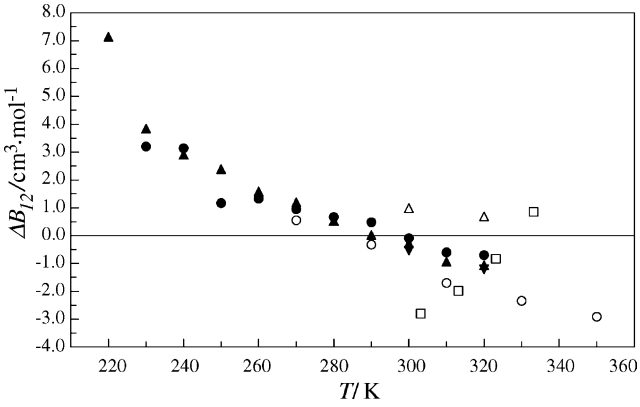

Fig. 10. Deviations between calculated and experimental interaction second virial coefficients. (△) for ($CH_4 + C_2H_6$) with data from [47]. (▼) for ($CH_4 + CO_2$) with data from [47]. (●) for ($CH_4 + CO_2$) with data from [50]. (◯) for ($N_2 + C_2H_6$) with data from [51]. (▲) for ($N_2 + CO_2$) with data from [50]. (□) for ($CO_2 + C_2H_6$) with data from [52].

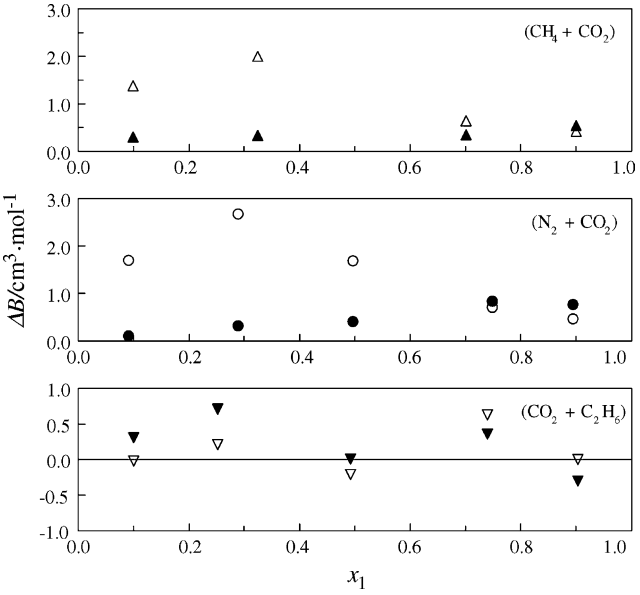

Fig. 11. Deviations between calculated and experimental mixture second virial coefficients at $T = 300$ K. Full markers are for results calculated with Model 2 (formal mixing rules) whereas open markers are for results calculated with the one-fluid mixture model (Model 1). (▲) and (△) for ($CH_4 + CO_2$) with data from [47]. (●) and (◯) for ($N_2 + CO_2$) with data from [49]. (▼) and (▽) for ($CO_2 + C_2H_6$) with data from [47].

AADs with both models are similar for all gas groups except for Group 3. For both models there are large deviations for the Group 3 samples N1, N10, N14, N16, N18, N20, N37, N51, N53, N54, N55, N56, N65, N66, N75 and N76 at $270 \leq T/\text{K} \leq 285$ and $6 \leq p/\text{MPa} \leq 12$, with average deviations reaching around 1.5% with Model 2 and around 1% with Model 4. The maximum deviations reached 5.4% with Model 2 and 3.9% with Model 4, in both cases at $T = 270$ K and $p = 11.9994$ MPa. Thus, the behaviour is analogous for both models regarding Group 3 gases but the effect is more pronounced with Model 2. Also, for sample RG2 [32,33] the maximum deviation occurs at $T = 275$ K and $p = 10.36$ MPa, being 1.48% with Model 2 and 1.05% with Model 4.

Regarding overall AADs in speeds of sound, the comparison of Models 2–4 is not favourable. There is a small relative increase in the overall AAD for natural gas systems, but there was a very significant relative increase for binary mixtures. There is an AAD of 1.0% with Model 2 for the system ($CH_4 + C_2H_6$) whereas it is 0.38% with Model 4. The largest deviations for both models occurred for the system ($0.50217CH_4 + 0.49783C_2H_6$) [27] on the isotherm $T = 275$ K at $6.5 \leq p/\text{MPa} \leq 11$, with deviations for Model 2 exceeding 10% and reaching a maximum of 28.8% at $p = 8.345$ MPa, whereas for Model 4 deviations were in excess of 2% for the same pressure interval with a maximum of 9.9% at $p = 8.087$ MPa. Also, from Table 4 we see that the AADs in u's for the other systems are more similar for both models yet smaller for Model 4.

The comparison of Models 1–2 is also quite favourable for the former. There is a small increase in the overall AAD for binary-mixture Z's. There is a very significant relative decrease in the overall AAD for natural-gas Z's and for binary-mixture u's and an important relative decrease in the overall AAD of natural-gas speeds of sound. In a similar manner, though to a lesser extent, the comparison of Models 3–4 is also favourable.

To summarise, we claim that out of the four models compared, Model 1 offers the best overall performance for the studied properties and systems. Apart from the AADs in binary-mixture Z's, deviations with Model 1 are the smallest in all the remaining categories given in Table 6. The proposed generalised virial-coefficient model of Eqs. (8)–(13), including the choice of reference fluid with the correct value of ω_0, is fundamental for the whole performance of the model, though that is mostly demonstrated by the very significant improvement in the prediction of pure-fluid properties shown in Tables 3 and 6. On the other hand, the use of the one-fluid mixture model resulted as well in a very important improvement in the prediction of natural-gas properties due to a better approximation to the mixture third virial coefficient. Clearly, Eq. (A.18) is based on pairwise additivity and this approximation is much less accurate for multicomponent mixtures than for binary systems. On the other hand, there is no particular gain from the use of the proposed virial-coefficient model with the mixture model of Eqs. (A.10)–(A.18). Also, the use of the Tsonopoulos [4] and Orbey and Vera [5] virial-coefficient models with the one-fluid mixture model is not interesting either given the large deviations in pure-fluid properties.

At this point it is important to highlight that the proposed virial model was fitted directly to primary experimental Z- and u-data of natural gas components, whereas the models of [4,5] were fitted mainly to derived quantities (B and C) for noble gases. We claim that, given the main objective of predicting primary properties of natural gas systems, the method used in this work is more systematic. Moreover, as we indi-

cated at the end of Section 3, the state-of-the-art *Z*-data from [16] are accurate within ±0.10%; therefore, fitting the model to these data enhances its predictive capability.

Although the amount of results presented in Figs. 1–6 is limited, they offer a view of the behaviour of Model 1. In Figs. 1 and 2 it is clear that the deviations tend to increase their range with the increase in the acentric factor of the fluid of interest, form $\omega = 0.011406$ for CH_4 to $\omega = 0.22491$ for CO_2. This appears to be typical corresponding-states behaviour. The same is seen in Figs. 3 and 4, in which the range of deviations increases with the difference in the acentric factors of the mixture components. Fig. 7 shows that the frequency distribution of AADs in compression factors is only slightly biased whereas the opposite occurs for the AADs in speeds of sound.

The results of Table 7 for deviations in pure-component virial coefficients seem to confirm the conclusions presented above. The overall deviations in pure-fluid second virial coefficients given in Table 7 for the proposed model are significantly smaller than those obtained with the Tsonopoulos [4] correlation. This is satisfactory given that the calculation was extended to fluids not included in the fitting of Eqs. (10)–(13) and extrapolated quite outside the custody transfer temperature interval. Moreover, the proposed virial model was fitted to *Z*- and *u*-data and not to second virial coefficient data as it was the model of [4]. Also, the overall deviation for third virial coefficients is higher than with the Orbey and Vera [5] correlation. We argue that this is due to the reduction in the number of adjustable coefficients from eight to six and the strong extrapolation in temperature.

The results of Table 8 show that deviations in calculated B_{mix} and C_{mix} are slightly higher with the proposed model than those with the correlations of [4,5]. This, again, might be due to the smaller number of adjustable coefficients in the proposed model. However, the extent of the deviations is in good agreement with the ordinary uncertainties of $\pm 1.5\ cm^3\ mol^{-1}$ in estimated B_{mix} and $\pm 300\ cm^3 \cdot mol^{-2}$ in estimated C_{mix}. The results of Table 9 also show slightly higher deviations in calculated ΔB_{12} and ΔC_{112} with the proposed model than those with the correlations of [4,5] whereas the inverse situation occurs in the case of ΔC_{122}. Again, the extent of these deviations is in good agreement with the expected uncertainties in the estimation of interaction virial coefficients.

Fig. 8 shows that deviations in calculated second virial coefficients are, on average, larger than the error bars. This is expected from not fitting Eqs. (10)–(13) to virial-coefficient data. Fig. 9 shows that, apart from lower temperatures, the average agreement between experimental and calculated third virial coefficients is relatively good.

The results of Fig. 11 illustrate that the mixture virial coefficients calculated with the one-fluid mixture model of Model 1 are not superior to those yielded by the formal mixing rules of Model 2. This is expected because the mixture model of Model 2 follows the formal composition dependence of Eqs. (2) and (3) whereas the one-fluid mixture model yields approximate mixture virial coefficients.

Finally, we compare the results of Model 1 to those of the virial EoS by Estela-Uribe et al. [1] and of the GERG virial EoS [2]. From [1], for the same fluids of Table 3, the overall AADs with the model of [1] were 0.017 and 0.15% for *Z*'s and *u*'s, respectively, while those with the model of [2] were 0.030 and 0.61%, respectively. For the same binary mixtures of Table 4, the overall AADs with the model of [1] were 0.018 and 0.25%, respectively for *Z*'s and *u*'s, whereas with the model of [2] the results were 0.027 and 1.01%, respectively. For natural gas systems, the overall AAD with the model of [1] for Groups 1–6 was 0.034 and for *u*'s the overall AAD was 0.17% for the same samples of Table 5; with the model of [2] the corresponding results were 0.039 and 0.81%, respectively. As expected, the results of Model 1 are not as good as those of [1,2] with regards to compression factors because a generalised model cannot match the performance of substance-specific models. However, the AADs with Model 1 for pure fluids and natural gas mixtures are not significantly larger than those of the model of [2] or even the model of [1]. On the other hand, it is very satisfactory that the overall AADs in speeds of sound with Model 1 are significantly smaller than those with the model of [1] for the three categories of systems studied. This is a consequence of the number of adjustable coefficients involved in the temperature derivatives of *B* and *C*. In Model 1 those derivatives involve eight adjustable coefficients while only four coefficients are involved in the model of [1]. In the model of [2] only two coefficients are involved in the first temperature derivatives and none in the second temperature derivatives.

5. Conclusions

The results we have presented are quite satisfactory within the objectives set up for this work. The proposed model, Model 1, achieved the objective of reducing the number of adjustable coefficients (from 17 for the models of [4,5] to 12) while improving on the overall predictive capability for pure-fluid and natural-gas densities and speeds of sound. The combination of the functional forms of Eqs. (8)–(13) and the one-fluid mixture model of Eqs. (14)–(20) is fundamental for these results. The one-fluid mixture model is a successful approximation to the description of mixture properties and in this work we used it to amend the unsatisfactory pairwise additivity approximation to the mixture third virial coefficient that is used in the models with formal mixing rules for the mixture virial coefficients. As expected, this worked well for the complex multicomponent mixtures of natural gas systems, but it showed its limitations in the case of binary-mixture densities and mixture second virial coefficients.

Finally, we expect improved results from the use of other combination of exponents in the virial-coefficient correlations. Also, a better approximation to the mixture third virial coefficient is needed to improve the predictive capability of models based on formal virial- coefficient mixing rules.

List of symbols

a,d,k	binary interaction parameters
b	coefficient in generalised second virial coefficient correlations
B	second virial coefficient
c	coefficient in generalised third virial coefficient correlations
C	third virial coefficient; heat capacity
n	amount of substance
p	pressure
r	radial separation between molecules
R	universal gas constant ($R = 8.31451\,\mathrm{J\,mol^{-1}\,K^{-1}}$)
T	temperature
u	speed of sound
x	mole fraction
Z	compression factor

Greek letters

ε	energy parameter of model intermolecular potential
ρ	amount-of-substance density
σ	distance parameter of model intermolecular potential
Φ	function of distance in model intermolecular potential

Superscripts

c	critical property
pg	perfect-gas property
res	residual property

Subscripts

i,j,k	component indices
mix	mixture property
r	reduced property
V	isochoric property

Acknowledgements

We thank Facultad de Ingeniería at Universidad Javeriana – Cali for financial support. Also, we are indebted to the students M.P. Camargo, R. Velasco and M. Zubieta for the organisation of some of the data used in this work.

Appendix A

A.1. Correlations for generalised second and third virial coefficients

The Tsonopoulos [4] correlation for the generalised second virial coefficient is

$$B = \left(\frac{RT^{\mathrm{c}}}{p^{\mathrm{c}}}\right)[B_0(T_{\mathrm{r}}) + \omega B_1(T_{\mathrm{r}})] \tag{A.1}$$

with

$$B_0(T_{\mathrm{r}}) = 0.1445 - \frac{0.330}{T_{\mathrm{r}}} - \frac{0.1385}{T_{\mathrm{r}}^2} - \frac{0.0121}{T_{\mathrm{r}}^3} - \frac{0.000607}{T_{\mathrm{r}}^8}, \tag{A.2}$$

and

$$B_1(T_{\mathrm{r}}) = 0.0637 + \frac{0.331}{T_{\mathrm{r}}^2} - \frac{0.423}{T_{\mathrm{r}}^3} - \frac{0.008}{T_{\mathrm{r}}^8}. \tag{A.3}$$

The Orbey and Vera [5] correlation for the generalised third virial coefficient is

$$C = \left(\frac{RT^{\mathrm{c}}}{p^{\mathrm{c}}}\right)^2[C_0(T_{\mathrm{r}}) + \omega C_1(T_{\mathrm{r}})], \tag{A.4}$$

with

$$C_0(T_{\mathrm{r}}) = 0.01407 + \frac{0.02432}{T_{\mathrm{r}}^{2.8}} - \frac{0.00313}{T_{\mathrm{r}}^{10.5}}, \tag{A.5}$$

and

$$C_1(T_{\mathrm{r}}) = -0.02676 + \frac{0.0177}{T_{\mathrm{r}}^{2.8}} + \frac{0.04}{T_{\mathrm{r}}^3} - \frac{0.003}{T_{\mathrm{r}}^6} - \frac{0.00228}{T_{\mathrm{r}}^{10.5}}. \tag{A.6}$$

A.2. Effective critical constants of quantum gases

The Gunn et al. [12] proposal for the effective critical temperature, pressure and density is

$$T^{\mathrm{c}} = \frac{T_0^{\mathrm{c}}}{1 + 21.8/MT}, \tag{A.7}$$

$$p^{\mathrm{c}} = \frac{p_0^{\mathrm{c}}}{1 + 44.2/MT}, \tag{A.8}$$

and

$$1/\rho^{\mathrm{c}} = v^{\mathrm{c}} = \frac{v_0^{\mathrm{c}}}{1 - 9.91/MT}. \tag{A.9}$$

in which T_0^{c}, p_0^{c} and v_0^{c} are the classical critical constants at high temperature and M is the molar mass. Values of the classical critical constants for quantum gases are given in [6].

A.3. Combining rules for pseudo-critical properties

Lee and Kesler [13] proposed combining rules for the interaction critical temperature T_{ij}^{c} and the interaction critical density ρ_{ij}^{c}:

$$T_{ij}^{\mathrm{c}} = (1 - k_{ij})(T_i^{\mathrm{c}} T_j^{\mathrm{c}})^{1/2}, \tag{A.10}$$

where k_{ij} is a binary interaction parameter, and:

$$\rho_{ij}^{c} = 8\left[\left(\frac{1}{\rho_i^c}\right)^{1/3} + \left(\frac{1}{\rho_j^c}\right)^{1/3}\right]^{-3}. \quad (A.11)$$

The interaction critical pressure is calculated from:

$$p_{ij}^{c} = Z_{ij}^{c}\rho_{ij}^{c}RT_{ij}^{c}. \quad (A.12)$$

Also, Lee and Kesler [13] proposed the following correlation for the interaction critical compression factor:

$$Z_{ij}^{c} = 0.291 - 0.08\omega_{ij}. \quad (A.13)$$

for which the interaction acentric factor is given by

$$\omega_{ij} = \tfrac{1}{2}(\omega_i + \omega_j). \quad (A.14)$$

In the case of mixtures containing quantum gases, the corrections to T_{ij}^{c} and p_{ij}^{c} are [12]:

$$T_{ij}^{c} = \frac{(1-k_{ij})(T_i^c T_j^c)^{1/2}}{1+(21.8/M_{ij}T)}. \quad (A.15)$$

and

$$p_{ij}^{c} = \frac{Z_{ij}^{c}\rho_{ij}^{c}R(1-k_{ij})(T_i^c T_j^c)^{1/2}}{1+(44.2/M_{ij}T)}. \quad (A.16)$$

with the interaction molar mass M_{ij} given by [6]:

$$M_{ij} = \frac{1}{2}\left[\frac{1}{M_i} + \frac{1}{M_j}\right]. \quad (A.17)$$

Finally, from the assumption of pairwise additivity, Orentlicher and Prausnitz [14] suggested the following approximation for the interaction virial coefficient C_{ijk}:

$$C_{ijk} = (C_{ij}C_{ik}C_{jk})^{1/3}, \quad (A.18)$$

in which C_{ij}, C_{ik} and C_{jk} are third virial coefficients corresponding to the interactions *i–j*, *i–k* and *j–k*, each of which is calculated with the procedure given for B_{ij}.

References

[1] J.F. Estela-Uribe, J. Jaramillo, J.P.M. Trusler, Fluid Phase Equilib. 204 (2003) 169–182.
[2] M. Jaeschke, S. Audibert, P. van Caneghem, A.E. Humphreys, R. Janssen-van Rosmalen, Q. Pellei, J.P.J. Michels, J.A. Schouten, C.A. ten Seldam, High accuracy compressibility factor calculation for natural gases and similar mixtures by use of a truncated virial equation, GERG Technical Monograph TM 2, 1989.
[3] K.E. Starling, J.L. Savidge, Compressibility factors of natural gas and other related hydrocarbon gases, AGA Transmission Measurement Committee Report 8, American Gas Association, 1992.
[4] C. Tsonopoulos, AIChE J. 20 (1974) 263–270.
[5] H. Orbey, J.H. Vera, AIChE J. 29 (1983) 107–113.
[6] J.M. Prausnitz, R.N. Lichtenthaler, E. Gomes de Azevedo, Molecular Thermodynamics of Fluid-phase Equilibria, 3rd ed., Prentice-Hall, 1999.
[7] K.S. Pitzer, D.Z. Lippman, R.F. Curl, C.M. Huggins, D.E. Petersen, J. Am. Chem. Soc. 77 (1955) 3433–3440.
[8] H. Orbey, Chem. Eng. Commun. 65 (1988) 1–19.
[9] K. Kis, H. Orbey, Chem. Eng. J. 41 (1989) 149–154.
[10] D.R. Schreiber, K.S. Pitzer, Fluid Phase Equilib. 46 (1989) 113.
[11] K.S. Pitzer, Fluid Phase Equilib. 59 (1990) 109–113.
[12] R.D. Gunn, P.L. Chueh, J.M. Prausnitz, AIChE J. 12 (1966) 937–941.
[13] B.I. Lee, M.G. Kesler, AIChE J. 21 (1975) 510–527.
[14] M. Orentlicher, J.M. Prausnitz, Can. J. Chem. 45 (1967) 373–378.
[15] Ch. Tegeler, R. Span, W. Wagner, J. Phys. Chem. Ref. Data 28 (1999) 779–850.
[16] M. Jaeshcke, A.E. Humphreys, The GERG databank of high accuracy compressibility factor measurements, GERG Technical Monograph TM4, 1990.
[17] J.P.M. Trusler, M.P. Zarari, J. Chem. Thermodyn. 24 (1992) 973–991.
[18] A.F. Estrada-Alexanders, J.P.M. Trusler, J. Chem. Thermodyn. 29 (1997) 991–1015.
[19] J.P.M. Trusler, M.P. Zarari, J. Chem. Thermodyn. 28 (1996) 329–335.
[20] S.J. Boyes, The Speed of Sound in Gases with Application to Equations of State and Sonic Nozzles, PhD Thesis, University of London, 1992.
[21] M.B. Ewing, J.P.M. Trusler, Physica A 184 (1992) 415–436.
[22] M.F. Costa-Gomes, J.P.M. Trusler, J. Chem. Thermodyn. 30 (1998) 527–534.
[23] A.F. Estrada-Alexanders, J.P.M. Trusler, J. Chem. Thermodyn. 30 (1998) 1589–1601.
[24] W.P. Clarke, Thermodynamic properties of N_2-Ar-O_2 mixtures from an extended corresponding states model, MSc Thesis, University of Idaho, 1990.
[25] S.M. Walas, Phase Equilibria in Chemical Engineering, Butterworth Publishers, 1985.
[26] M. Jaeschke, P. Schley, Int. J. Thermophys. 16 (1995) 1381–1392.
[27] B.A. Younglove, N.V. Frederick, R.D. McCarty, Speed of sound data and related models for mixtures of natural gas constituents, National Institute of Standard Technology (U.S.) Monograph 178, 1993.
[28] J.P.M. Trusler, J. Chem. Thermodyn. 26 (1994) 751–763.
[29] J.P.M. Trusler, M.F. Costa-Gomes, The speed of sound in methane and in two methane-rich gas mixtures, Report to the GERG Working Group 1.3, 1996.
[30] J.P.M. Trusler, W.A. Wakeham, M.P. Zarari, High Temp. High Press. 25 (1993) 291–296.
[31] J.F. Estela-Uribe, Equation of State for Natural Gas Systems, PhD Thesis, University of London, 1999.
[32] J.W. Magee, W.M. Haynes, M.J. Hiza, J. Chem. Thermodyn. 29 (1997) 1439–1454.
[33] C.-A. Huang, P.P. Simon, H. Hou, K.R. Hall, J.C. Holste, K.N. Marsh, J. Chem. Thermodyn. 29 (1997) 1455–1472.
[34] J.H. Dymond, E.B. Smith, The virial coefficients of pure mixtures, Oxford University Press, 1980.
[35] R. Gilgen, R. Kleinrahm, W. Wagner, J. Chem. Thermodyn. 26 (1994) 383–398.
[36] P. Nowak, R. Kleinrahm, W. Wagner, J. Chem. Thermodyn. 29 (1997) 1137–1156.
[37] W. Duschek, R. Kleinrahm, W. Wagner, J. Chem. Thermodyn. 22 (1990) 827–840.
[38] R. Kleinrahm, W. Duschek, W. Wagner, M. Jaeschke, J. Chem. Thermodyn. 20 (1988) 621–631.
[39] G. Händel, R. Kleinrahm, W. Wagner, J. Chem. Thermodyn. 24 (1992) 685–695.
[40] D.R. Douslin, R.H. Harrison, J. Chem. Thermodyn. 5 (1973) 491–512.
[41] M. Funke, R. Kleinrahm, W. Wagner, J. Chem. Thermodyn. 34 (2002) 2001–2015.
[42] R.H.P. Thomas, R.H. Harrison, J. Chem. Eng. Data 27 (1982) 1–11.
[43] M.B. Ewing, A.R.H. Goodwin, J. Chem. Thermodyn. 23 (1991) 1107–1120.

[44] M.B. Ewing, A.R.H. Goodwin, M.L. McGlashan, J.P.M. Trusler, J. Chem. Thermodyn. 20 (1988) 243–256.
[45] M.B. Ewing, A.R.H. Goodwin, J. Chem. Thermodyn. 24 (1992) 301–315.
[46] M.B. Ewing, A.R.H. Goodwin, J.P.M. Trusler, J. Chem. Thermodyn. 21 (1989) 867–877.
[47] H. Hou, J.C. Holste, K.R. Hall, K.N. Marsh, B.E. Gammon, J. Chem. Eng. Data 41 (1996) 344–353.
[48] P.J. McElroy, J. Fang, J. Chem. Thermodyn. 26 (1994) 617–623.
[49] H.B. Brugge, C.-A. Hwang, W.J. Rogers, J.C. Holste, K.R. Hall, W. Lemming, G.J. Esper, K.N. Marsh, B.E. Gammon, Physica A 156 (1989) 382–416.
[50] G.J. Esper, D.M. Bailey, J.C. Holste, K.R. Hall, Fluid Phase Equilib. 49 (1989) 35–47.
[51] H.J. Achtermann, G. Magnus, H.M. Hinze, M. Jaeschke, Fluid Phase Equilib. 64 (1991) 263–280.
[52] P.J. McElroy, M.K. Dowd, R. Battino, J. Chem. Thermodyn. 22 (1990) 505–512.
[53] L.A. Weber, Int. J. Thermophys. 13 (1992) 1011–1032.